Acta Cryst. (1997). D53, 311–315

The First Structure at 1.8 Å Resolution of an Active Autolysate Form of Porcine α-Trypsin

A. JOHNSON,[a] S. KRISHNASWAMY,[b] P. V. SUNDARAM[c] AND VASANTHA PATTABHI[a]*

[a]*Department of Crystallography and Biophysics, University of Madras, Madras – 600 025, India,* [b]*Bioinformatics Centre, School of Biotechnology, Madurai – Kamaraj University, Madurai – 625 021, India, and* [c]*Centre for Protein Engineering and Bio-medical Research, The Voluntary Health Service, Madras – 600 113, India. E-mail: crystal@giasmd01.vsnl.net.in*

(Received 25 July 1996; accepted 9 January 1997)

Abstract

The first crystal structure of an active autolysate form of porcine α-trypsin (APT), a two-chain molecule obtained from the limited autolysis of porcine β-trypsin at position Lys145–Ser146, has been determined. APT crystallizes in space group $P2_12_12_1$ with one protein molecule in the asymmetric unit. The structure was solved by molecular replacement followed by refinement using *X-PLOR* to an *R* factor of 0.200 and an R_{free} of 0.285 for 8.0–1.8 Å data with r.m.s. deviations from ideal values of 0.01 Å and 1.7° for bond lengths and bond angles, respectively. Comparison with inactive autolysate porcine ε-trypsin (EPT) and porcine β-trypsin in complex with bittergourd trypsin inhibitor (MCT) revealed a small but systematic directional chain shift around the active-site residues from APT to EPT to MCT.

1. Introduction

Serine proteinases are of considerable importance in catalyzing many biological processes. Their roles span from basic functions in digestion to key regulatory mechanisms such as peptide hormone release, coagulation and complement activation (Reich, Riffkin & Shaw, 1975; Ribbons & Brew, 1976). The active centre of porcine trypsin, a serine proteinase, is a charge-transfer catalytic triad composed of His57, Ser195 and Asp102. Guo, Guan & Zhang (1985) isolated three autolysates of porcine β-trypsin, a double-chain δ-trypsin which is cleaved at position Arg117–Val118, a three-chain γ-trypsin with breaks at Lys159–Ala160 and Arg117–Val118, and a three-chain σ-trypsin cleaved at Lys159–Ala160 and Lys145–Ser146. These three autolysates still had trypsin activity against benzoyl-L-arginine ethyl ester (BAEE). Huang, Wang, Li, Liu & Tang (1994) reported the only crystal structure of a trypsin autolysate named porcine ε-trypsin (EPT) which is inactive and has breaks at Lys60–Ser61 and Lys145–Ser146. APT, reported in this paper, is a double-chain porcine trypsin with a break at Lys145–Ser146 and has trypsin activity against benzoyl arginine *p*-nitroanilide (BAPNA) (Erlanger, Kokowsky & Cohen, 1961).

Most crystal structures of trypsin are those of inhibited enzymes because during the course of crystallization, uninhibited enzymes undergo autolysis and then cause the crystallization to fail. Therefore, it is interesting to compare the structure of the active autolysate reported here with those of the inactivated autolysate EPT and porcine β-trypsin complexed with bittergourd inhibitor (MCT) (Huang, Liu & Tang, 1994).

2. Experimental

2.1. *Crystallization and data collection*

APT was obtained from limited autolysis of porcine β-trypsin purchased from Sigma Chemical Company, St Louis, MO, USA (Schroeder & Shaw, 1969). The activity of the enzyme was assayed by the standard method (Erlanger *et al.*, 1961) after incubation at an elevated temperature for a designated period of time with BAPNA as substrate. The crystals were grown at 293 K by vapour diffusion using the hanging-drop technique. The drop contained 15 mg ml^{-1} of protein and 20 m*M* $CaCl_2$ in 0.05 *M* sodium acetate buffer pH 6.7. The precipitant and reservoir solutions were 0.04 *M* and 1.5 *M* ammonium sulfate in the same buffer. The precipitant and the protein solutions were mixed in the ratio of 1:1 in the hanging drop. Needle-shaped crystals were obtained after one week. The size of the crystal used for data collection was 0.1 × 0.3 × 1.6 mm and it diffracted up to a resolution of 1.8 Å. The cell constants are $a = 77.70$, $b = 53.82$, $c = 47.08$ Å. The space group is $P2_12_12_1$ with $Z = 4$ and $V = 1.97 \times 10^5$ Å^3. The diffraction data were collected on a MAR Research X-ray imaging system, processed and scaled using *MarXDS*. Data-collection statistics are given in Table 1.

2.2. *Structure solution and refinement*

The crystal structure was solved by the molecular replacement method (Huber, 1985; Rossman & Blow, 1962) using *X-PLOR*. Since the APT crystals were isomorphous with those of EPT, the search model consisted of the coordinates of porcine β-trypsin in MCT placed in the EPT unit cell. EPT itself was not used as a model in order to eliminate bias in the positions

Table 1. *Data collection statistics*

The values of R and R_{free} for the refined structure are also indicated.

Resolution range (Å)	No. of reflections measured	No. of unique reflections $F \geq 1\sigma(F_o)$	Percentage completion	R_{merge} (%)	R value	R_{free}
8.0–6.0	924	295	92.8	4.8	0.26	0.32
6.0–4.0	3852	1223	95.5	5.1	0.14	0.24
4.0–3.5	2599	833	96.7	7.6	0.14	0.22
3.5–2.8	7617	2401	96.5	10.3	0.19	0.31
2.8–2.5	6282	1921	95	18.6	0.24	0.27
2.5–2.25	7970	2459	94.5	23.9	0.26	0.30
2.25–2.0	12181	3769	93	35.1	0.26	0.30
2.0–1.8	15077	4585	91.3	66.1	0.27	0.31
Total	56502	17486	95	8	0.20	0.28

of the chain breaks. A consistent solution at Eulerian angles $\theta_1 = 0.0$, $\theta_2 = 0.0$, $\theta_3 = 0.0°$ and translation $\delta X = 0.0$, $\delta Y = 0.0$, $\delta Z = 0.0$ appeared in five different resolution ranges. The initial R factor for data in the resolution range 8.0–2.5 Å with 2σ cut-off in F was 0.426. Rigid-body refinement and positional refinement using *X-PLOR* resulted in a model with an R factor of 0.282 and R_{free} of 0.372. Subsequently a cycle of simulated-annealing refinement (Brünger, Kuriyan & Karplus, 1987; Brünger, Krukowski. & Erickson, 1990) reduced the R factor to 0.222. The structure was further refined using 8.0–2.0 Å data and the model was corrected using $(2F_o - F_c)$ and $(F_o - F_c)$ maps employing *TURBO FRODO* (Jones, 1978). The autolysis site was confirmed using omit maps. A total of 111 solvent molecules were added at stereochemically reasonable positions with the help of $(2F_o - F_c)$ and $(F_o - F_c)$ maps. Even though the R_{merge} for the reflections in the resolution range 2.0–1.8 Å was high they were also included in refinement calculations as this is known to improve the electron density (Dodson, Kleywegt & Wilson, 1996). All reflections with $F \geq \sigma(F)$ were used in the final cycles. The refinement terminated at $R = 0.200$, $R_{free} = 0.285$. The final refinement characteristics are given in Table 2. The structure solution, fitting and refinement were performed on a Silicon Graphics Crimson/Elan system. The final refined coordinates have been deposited with the Brookhaven Protein Data Bank*

3. Results and discussion

3.1. *Overall structure*

The overall structural features of APT are very similar to those of EPT and the trypsin molecule in MCT and trypsin complexed with the inhibitor 2-amino methyl cyclohexane (TNG) (Kurinov & Harrison, 1994). The main-chain atoms of APT superposes on those of the other three structures with r.m.s. deviations of 0.27, 0.47

Table 2. *Final refinement parameters*

Resolution range (Å)	8.0–1.8
No. of unique reflections used for refinement	17486
No. of protein atoms	2032
Calcium	1
Water O atoms	111
R value	0.200
Free R	0.285
R.m.s. deviations from ideal geometry	
Bond length (Å)	0.01
Bond angle (°)	1.7
Torsion angle (°)	26.9
Improper angle (°)	1.5
Estimated mean coordinate error (Luzzati, 1952)	0.2

and 0.46 Å, respectively. The Ramachandran plot for the structure is given in Fig. 1. While most of the amino-acid residues are in the allowed regions (Ramachandran, Ramakrishnan & Sasisekaran, 1963), a few of them have φ–ψ angles outside the allowed regions as is also the case with other known homologous trypsin structures.

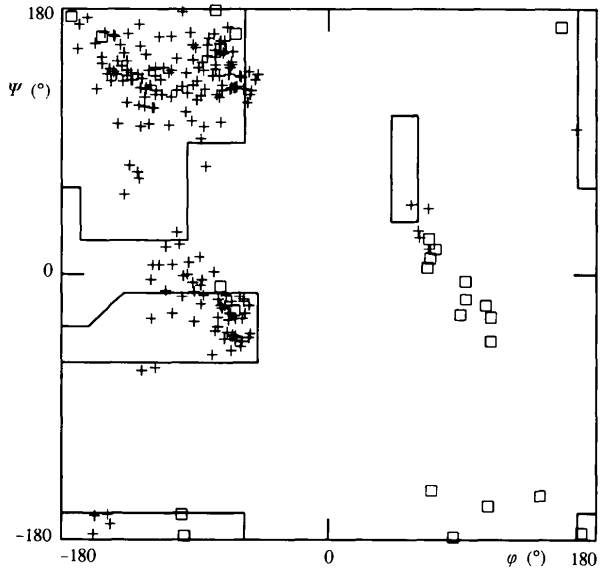

Fig. 1. Ramachandran plot for the main-chain torsion angles. Glycine residues are shown as squares. This figure and Figs. 2 and 3 were prepared using *TURBO FRODO* (Jones, 1978).

* Atomic coordinates and structure factors have been deposited with the Protein Data Bank, Brookhaven National Laboratory (Reference: 1AKS, R1AKSSF). Free copies may be obtained through The Managing Editor, International Union of Crystallography, 5 Abbey Square, Chester CH1 2HU, England (Reference: VJ0006).

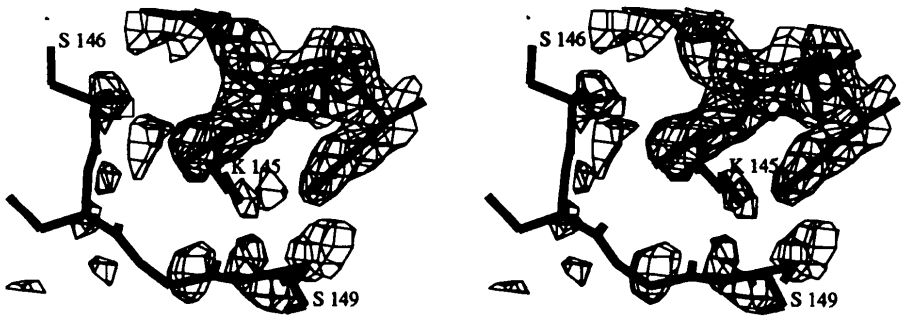

Fig. 2. Stereoview of the $2F_o - F_c$ map around the autolysis site Lys145–Ser146 of APT.

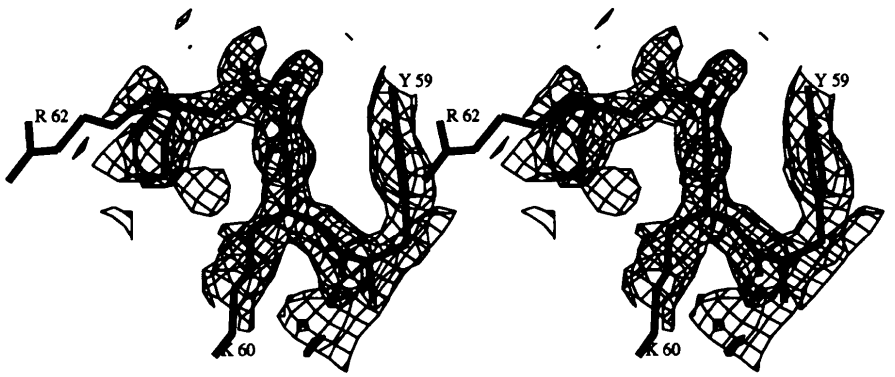

Fig. 3. Stereoview of the $2F_o - F_c$ map around Lys60–Ser61.

The comparison indicates that these homologous structures differ from one another in minor details but their overall conformation is the same. However, systematic chain shifts, though small, are observed at a few places between APT, EPT and MCT.

The final $2F_o - F_c$ and $F_o - F_c$ electron-density maps show a break after Lys145. The density could be seen again from Ser150. The region Ser146–Ser150 was included in the model in the final stages and they gained weak electron density (Fig. 2). A similar situation was observed in the case of EPT which has one break at Lys145–Ser146 in addition to that at Lys60–Ser61. However in APT which is active, the Lys60–Ser61 is not lysed as seen from the electron density (Fig. 3). The autolytic site is marked by an abnormally high temperature factor as can be seen from Fig. 4 which illustrates the variations of B along the polypeptide chain. The calcium-binding site is quite important for the integrity of the trypsin structure and the calcium ion is bound almost in the same manner in APT, EPT and MCT.

3.2. *Active site*

APT is 80% as active as porcine β-trypsin. The hydrogen-bond geometry around the active centre is similar to that in EPT, MCT and TNG. There seems to be a directional relative shift of residues (Fig. 5) in regions L1 (residues 32–44), L2 (residues 54–60), L3 (residues 64–103), L4 (residues 151–157) and L5 (residues 191–197) around the active site of APT when compared with EPT and MCT. On the whole these residues are father away from the centre of the active site in APT than in EPT. Those in MCT are closest to the centre. This pattern of shift can also be discerned from Fig. 6 which illustrates the atomic positions in the three structures in a sphere of 8 Å radius around the centre of the active site. It can also be seen from this

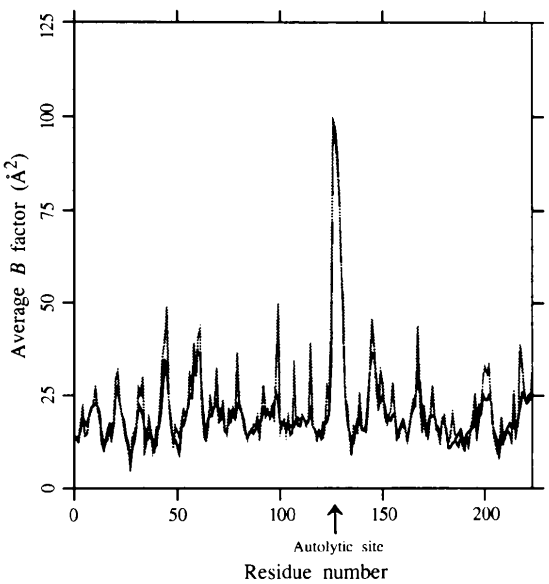

Fig. 4. Temperature factors averaged for the side-chain (dotted) and main-chain (thick line). This figure and Figs. 5 and 6 were prepared using *Insight*II (Biosym Inc., 1993).

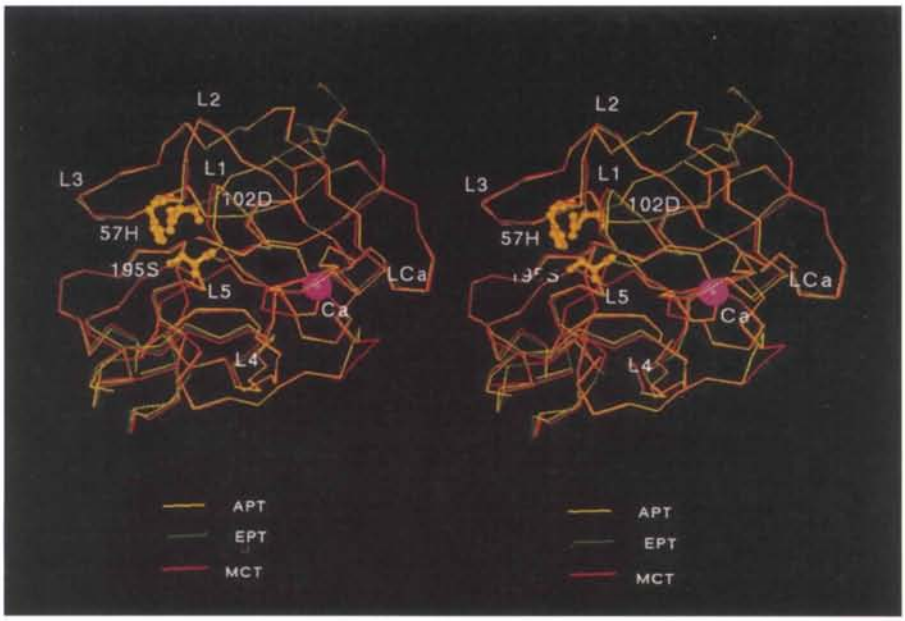

Fig. 5. Superposition of the C^{α} traces of APT (yellow line), EPT (green line) and MCT (red line). Active-site residues are shown in ball-and-stick representation. See text for details.

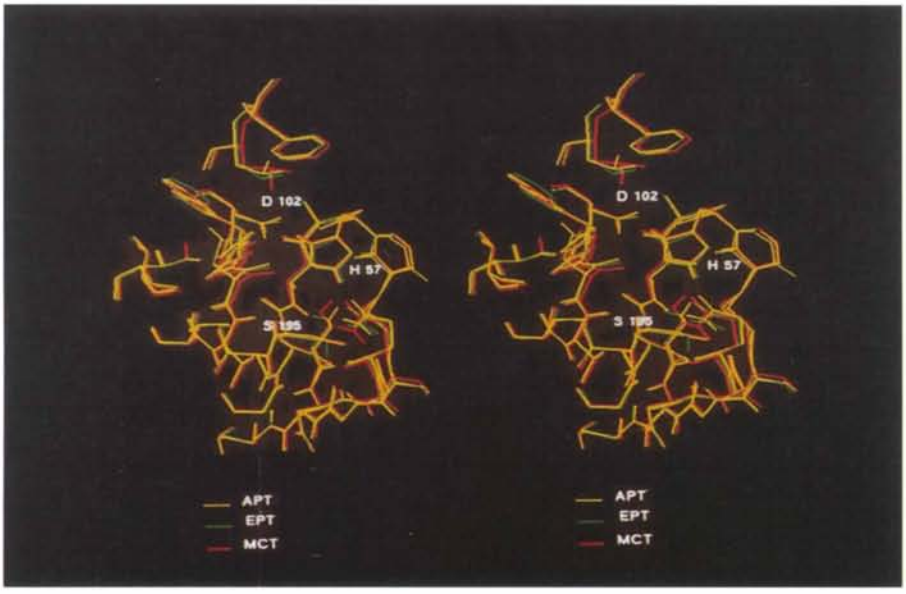

Fig. 6. Comparison of atoms within a sphere of 8 Å around the active site of APT (yellow line), EPT (green line) and MCT (red line).

figure that autolysis at Lys145–Ser146 does not affect the conformation of the active center. Another interesting observation pertains to the temperature factor of Leu99 which is at the entrance of the active site. The value is high in APT (18 $Å^2$) as in other inhibited active trypsin forms ($\simeq$16 $Å^2$) while it is very low (2 $Å^2$) in EPT. Thus, the flexibility of residue Leu99, the intact Lys60–Ser61 bond and the systematic shift referred to above may be responsible for the activity of this autolysate.

PVS and the Centre for Protein Engineering and Biomedical Research are funded by the Department of Biotechnology, Government of India. We acknowledge the use of National Facility for High Resolution Silicon Graphics, Bioinformatics centre, Madurai Kamaraj University and National Facility for Macromolecular data collection at IISc., Bangalore. We thank Dr N. Gautham for useful discussions and help.

References

Biosym Inc. (1993). *Insight*II. Biosym Inc., San Diego, CA, USA.

Brünger, A. T., Krukowski, A. & Erickson, J. (1990). *Acta Cryst.* A**46**, 585–593.

Brünger, A. T., Kuriyan, J. & Karplus, M. (1987). *Science*, **235**, 458–460.

Dodson, E., Kleywegt, G. J & Wilson, K. (1996). *Acta Cryst.* D**52**, 228–234.

Erlanger, K. E., Kokowsky, N. & Cohen, W. (1961). *Arch. Biochem. Biophys.* **95**, 271–278.

Guo, H., Guan, Y. & Zhang, L. (1985). *Chin. Biochem. J.* **1**, 53–59.

Huang, Q., Liu, S. & Tang, Y. (1994). *J. Mol. Biol.* **229**, 1022–1036.

Huang, Q., Wang, Z., Li, Y., Liu, S. & Tang, Y. (1994). *Biochim. Biophys. Acta*, **1209**, 77–82.

Huber, R. (1985). *Proceedings of the Daresbury Study Weekend*, pp. 58–61. Warrington: Daresbury Laboratory.

Jones, T. A. (1978). *J. Appl. Cryst.* **11**, 268–272.

Kurinov, I. & Harrison, R. W. (1994). *Nature Struct. Biol.* **1**, 735–743.

Luzzati, V. (1952). *Acta Cryst.* **5**, 802–810.

Reich, E., Riffkin, D. B. & Shaw, E. (1975). *Proteinases and Biological Control*, Vol. 2. New York: Cold Spring Harbor Laboratory Press.

Ribbons, D. W. & Brew, K. (1976). *Proteolysis and Physiological Regulation*. New York/London: Academic Press.

Rossmann, M. G. & Blow, D. M. (1962). *Acta Cryst.* **15**, 24–31.

Ramachandran, G. N., Ramakrishnan, C. & Sasisekaran (1963). *J. Mol. Biol.* **7**, 95–99.

Schroeder, D. D. & Shaw, E. (1969). *J. Mol. Chem.* **243**, 2943–2949.